


 Cite this: *RSC Adv.*, 2022, 12, 18301

# Explanation for the selective crystallization from inosine solutions using mid-frequency Raman difference spectra analysis†

 Fenghua Chen,<sup>a</sup> Chenmei Yang,<sup>a</sup> Xinyu Cheng,<sup>b</sup> Yingjie Fan,<sup>b</sup> Xinyuan Chen,<sup>b</sup> Shizhao Ren<sup>\*a</sup> and Rongrong Xue<sup>ib\*</sup>

Mid-frequency Raman difference spectra (MFRDS) analysis can be used to reveal the selective crystallization from solutions through determining the degree of similarity of the short-range orders between the assemblies of small organic molecules in solutions and their solid phases. Four solid phases of inosine (IR) ( $\alpha$ -anhydrous IR ( $\alpha$ -IR),  $\beta$ -anhydrous IR ( $\beta$ -IR), IR dihydrate (IRD), and amorphous IR (AmIR)) and two IR solutions (aqueous and 70 vol% DMSO aqueous solution) were prepared and characterized using MFRDS here. The MFRDS analysis results indicate that the selective formation of IRD and AmIR from IR aqueous solution and  $\beta$ -IR from IR 70 vol% DMSO solution are originated from the high similarity of their short-range structures. Moreover, we propose that the formation of  $\alpha$ -IR from IR aqueous solution benefits from the appearance of AmIR as an intermediate phase. MFRDS is a robust tool to explain and predict the possible precipitation products from various solutions of small organic molecules.

 Received 3rd May 2022  
Accepted 15th June 2022

DOI: 10.1039/d2ra02797f

[rsc.li/rsc-advances](https://rsc.li/rsc-advances)

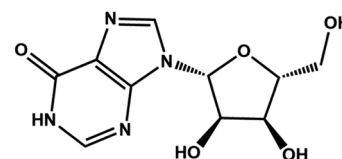
## 1 Introduction

The outcome predictions of crystallization processes in classical nucleation theory (CNT) and non-classical nucleation theory (NCNT) are amazing fields.<sup>1–4</sup> Numerous studies have been carried out to explain and predict the crystallization polymorphs under different experimental conditions. The short-range orders of small organic molecules in specified solutions, especially the molecular self-assemblies, may play a key role in determining the selective crystallization polymorphs from solutions. It is necessary and still a big challenge to establish an effective method to reveal the inherent relationship between precursors and crystallized products from solutions.

Raman spectroscopy is a powerful tool to determine the molecular structure, molecular conformation, intermolecular interactions, and molecular packing pattern, all of which are strongly related to the short-range orders of organic molecules. Low-frequency Raman spectra (LFRS,  $\leq 300\text{ cm}^{-1}$ ) can be used to distinguish different polymorphs of organic molecules,<sup>5–8</sup> as Raman peaks below  $300\text{ cm}^{-1}$  are phonon modes contributed to the unit cell motions (lattice vibrational frequencies).<sup>9</sup> And mid-frequency Raman spectra (MFRS,  $300\text{--}1800\text{ cm}^{-1}$ ) can provide information about the short-range orders of organic molecules

both in solutions and solid states.<sup>5</sup> Thus, the similarity between the short-range orders of small organic molecules in specified solutions and solid phases can be determined by analyzing the similarity of MFRS of them. However, it is sometimes subjective and difficult to determine the degree of similarity between multiple MFRS by only visual observation, which may lead to unreasonable or uncertain results. Meanwhile, one or multiple characteristic peaks could not represent the total short-range orders of assemblies of organic molecules in solutions or organic solids. A more intuitive and even quantitative analysis method is needed. Mid-frequency Raman difference spectra (MFRDS) can directly show the differences between MFRS of two polymorphs, and the smoother the MFRDS are, the more similar short-range orders they have. The average deviation (a.d., the average value of absolute value of the intensity of MFRDS) and standard deviation (s.d.) of all the data in the MFRDS can be used to semi-quantitatively describe the degree of similarity.

Inosine (IR) molecule contains a rigid ring and a flexible ribofuranosyl group as shown in Scheme 1. Intramolecular rotations, especially in the part of ribofuranosyl,<sup>10</sup> could induce



Scheme 1 Molecular structure of inosine (IR).

<sup>a</sup>School of Resources and Chemical Engineering, Sanming University, Sanming 365004, Fujian, China. E-mail: [rensz@fj-smu.edu.cn](mailto:rensz@fj-smu.edu.cn); [rongrongxue@fj-smu.edu.cn](mailto:rongrongxue@fj-smu.edu.cn)
<sup>b</sup>College of Environmental Science and Engineering, Fujian Normal University, Fuzhou 350007, Fujian, China

 † Electronic supplementary information (ESI) available: Additional Raman spectra, and tables. See <https://doi.org/10.1039/d2ra02797f>


rich conformations of IR molecule, which are beneficial for the formation of various solid phases of IR. There are three common polymorphs of IR,  $\alpha$ -anhydrous IR ( $\alpha$ -IR, the commercial raw IR),<sup>11</sup>  $\beta$ -anhydrous IR ( $\beta$ -IR, the most stable polymorph),<sup>11–13</sup> and IR dihydrate (IRD).<sup>14</sup> The rich crystallization behavior makes IR a good model molecule to study the relationship between the selectivity of solution crystallization process and the degree of similarity of the short-range orders between organic molecular assemblies in solutions and the corresponding solution crystallization products. For the solution crystallization of IR,  $\alpha$ -IR can be prepared by recrystallization in water at room temperature,<sup>11</sup> IRD can be obtained from IR aqueous solution below 10 °C,<sup>14</sup> and amorphous IR (AmIR) can be prepared by spray drying IR aqueous solution through a non-classic nucleation process, as reported in our recent work (Xue *et al.*, Explanation and Prediction for the Selective Recrystallization of Amorphous Phases and Dehydration Process of Hydrates by Using Raman Difference Spectra: Guanosine and Inosine, submitted). And  $\beta$ -IR can be crystallized from 70 vol% DMSO aqueous solution.<sup>15</sup> It has been reported that the initial nucleation of  $\alpha$ -IR from aqueous solution at temperature above 10 °C is directed by dimeric self-association demonstrated by proton nuclear magnetic resonance, but the crystallization of IRD from aqueous solution at lower temperatures could not be explained in the same way.<sup>16</sup> The detailed relationships between different IR solutions and solids have not been established yet.

In this work, different solid phases of IR ( $\alpha$ -IR,  $\beta$ -IR, IRD, and AmIR), saturated aqueous solution of IR (IR-AQ), and saturated 70 vol% DMSO aqueous solution of IR (IR-DMSO) were prepared and characterized by MFRS. Further, the MFRS of solute IR in different solutions (IR in IR-AQ: IR-AQD, IR in IR-DMSO: IR-DMSOD) were calculated by subtracting the Raman signal of solvents from the MFRS of the corresponding solutions. MFRDS analysis results of different solid phases and solutions of IR indicate that IR molecules in aqueous solution has the most similar short-range orders with AmIR among all IR solids and the most similar short-range orders with IRD among all IR crystals. We propose that IRD can be selectively crystallized from IR aqueous solution through CNT process, and  $\alpha$ -IR can be obtained from IR aqueous solution after the formation and crystallization of AmIR by NCNT process. The analysis results are consistent with the reported crystallization phenomena well. Moreover, MFRDS analysis results indicate that IR molecules in 70 vol% DMSO aqueous solution has the most similar short-range orders with AmIR among all IR solids and the most similar short-range orders with  $\beta$ -IR among all IR crystals, which can explain the selective recrystallization of  $\beta$ -IR from 70 vol% DMSO and indicate that AmIR might be obtained from IR 70 vol% DMSO aqueous solution. As DMSO is a kind of solvent with high boiling point, we cannot obtain AmIR from IR-DMSO by removing solvents quickly. However, we found that  $\alpha$ -IR can also be obtained which might form *via* an amorphous intermediate phase from IR-DMSO by providing a high supersaturation. We propose that MFRDS analysis is a feasible method to explain and predict the possible precipitation products from various solutions of small organic molecules.

## 2 Experimental

### 2.1 Materials

Inosine (C<sub>10</sub>H<sub>12</sub>N<sub>4</sub>O<sub>5</sub>, 98%,  $\alpha$ -IR) was bought from Aladdin. NaCl (99.5%) and ammonia water (NH<sub>3</sub>·H<sub>2</sub>O, AR) were bought from Xilong Scientific. Dimethyl sulfoxide (DMSO, C<sub>2</sub>H<sub>6</sub>OS, AR) was bought from Sinopharm.

### 2.2 Methods

**2.2.1 Preparation of different solid phases and solutions of IR.** AmIR was prepared by ball milling the mixture of 1 g raw IR and 1 g NaCl,  $\beta$ -IR was recrystallized from 70 vol% DMSO aqueous solution (the solution was cooled from 60 °C to room temperature), and IRD was recrystallized from ammonia solution by ammonia volatilization at 10 °C. Saturated aqueous solution of IR (IR-AQ) and saturated 70 vol% DMSO aqueous solution of IR (IR-DMSO) were obtained by filtering the supernatant of the corresponding saturated IR solution with a filter membrane (pore size: 0.22  $\mu$ m for aqueous solution and 0.45  $\mu$ m for 70 vol% DMSO aqueous solution).

**2.2.2 Raman spectroscopy test.** Samples obtained in this work were characterized by confocal Raman spectroscopy (Thermo Fisher Scientific, DXR3xi, 532 nm laser, 40 mW laser power, 1000 scan times, 50 to 3400 cm<sup>-1</sup>, 50 $\times$  objective lens). The exposure time varies for different samples: 20 Hz for IR-AQ and water (AQ, a small amount of NaCl was added to obtain acceptable Raman signals because it is difficult to obtain the Raman spectra of pure water), 200 Hz for  $\alpha$ -IR,  $\beta$ -IR and IRD, 600 Hz for AmIR, DMSO, and IR-DMSO.

**2.2.3 Raman spectra data processing.** Raman spectra of all the samples were normalized for MFRDS analysis. I<sub>1552</sub> of  $\alpha$ -IR, I<sub>1545</sub> of  $\beta$ -IR, I<sub>1553</sub> of IRD and IR-AQ, I<sub>1548</sub> of AmIR, and I<sub>673</sub> of DMSO and IR-DMSO were used for normalization, respectively. The MFRS of solute IR in different solutions were calculated by subtracting the Raman signal of solvents from the MFRS of the corresponding solutions. IR-AQD is the difference spectrum of IR-AQ with AQ (both normalized by I<sub>1639</sub>), and then normalized by I<sub>1553</sub>. IR-DMSOD is the difference spectrum of IR-DMSO with DMSO (both normalized by I<sub>673</sub>), and then normalized by I<sub>1545</sub>. MFRDS with baseline deduction are carried out in the same way except for one pre-processing step: baseline deduction based on a polynomial fitting method.

## 3 Results and discussion

### 3.1 MFRDS analysis of IR-AQD with IR solids

Since valid Raman signals of IR solutions can only be obtained with high-energy laser, laser with wavelength of 532 nm, instead of 785 nm that was always used in our work, was used here. Four IR solids ( $\alpha$ -IR,  $\beta$ -IR, IRD, and AmIR) were prepared by mature methods, which were confirmed with the LFRS results (Fig. S1, Table S1†). As reported in our recent work (Xue *et al.*) that AmIR prepared by different methods has very similar Raman spectra, AmIR prepared by ball milling method was used in this work. The MFRS of  $\alpha$ -IR,  $\beta$ -IR, IRD, and AmIR are shown in Fig. 1a. And the MFRS of IR-AQ (Fig. 1b) obviously shows the



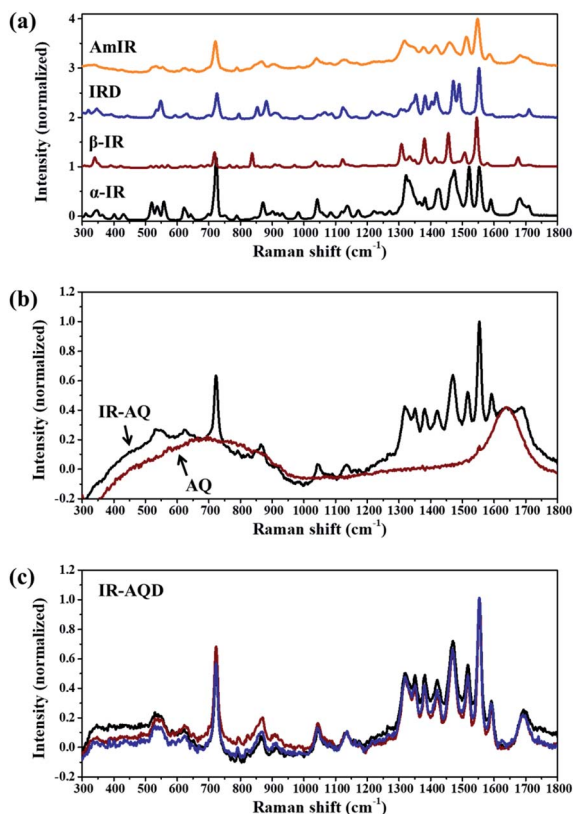


Fig. 1 Mid-frequency Raman spectra (MFRS, in the range of 300–1800  $\text{cm}^{-1}$ ) of (a)  $\alpha$ -IR,  $\beta$ -IR, IRD, and AmIR, (b) IR-AQ and AQ, and (c) IR-AQD (the results of three parallel tests are shown here).

characteristic signals of IR and solvent (AQ). The LFRS of IR-AQ shows obvious amorphous features, and its high-frequency Raman spectrum (HFRS, 2600–3400  $\text{cm}^{-1}$ ) mainly shows the signals of AQ (Fig. S2<sup>†</sup>). The MFRS of IR in aqueous solution (IR-AQD, Fig. 1c) was obtained by subtracting the Raman signal of AQ from the MFRS of IR-AQ. IR-AQD shows the signals originated from the interaction between IR molecules or IR and water molecules.

The similarity of short-range orders between IR assemblies in its saturated aqueous solution and different IR solids ( $\alpha$ -IR,  $\beta$ -IR, IRD, and AmIR) were studied by analyzing the similarity of their Raman spectra. As it is difficult to determine the degree of similarity between the MFRS of IR-AQD and the four IR solids by only visual observation, MFRDS analysis (Fig. 2 and S3<sup>†</sup>) were used to describe their similarity quantitatively. The corresponding a.d. and s.d. are shown in Table 1. And the MFRDS analysis results of every IR solids and IR-AQD with themselves are shown in Table S2.<sup>†</sup> In the process of MFRDS analysis, we found that the existence of inherent baseline fluctuations would seriously interfere with the results, and thus a baseline deduction based on a polynomial fitting method was introduced into the MFRDS analysis process to eliminate the interference of baseline. The MFRDS obtained with baseline deduction, show a better parallelism. The a.d. and s.d. of the MFRDS with baseline deduction are smaller, especially for the MFRDS of AmIR with IR-AQD. We used the analysis results of MFRDS with baseline deduction for

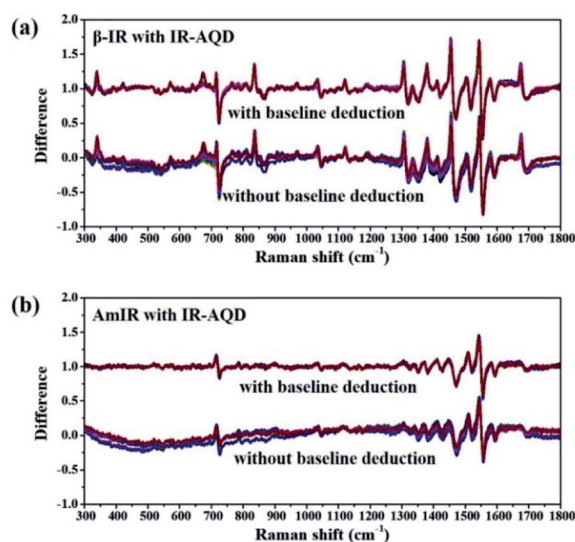


Fig. 2 Mid-frequency Raman difference spectra (MFRDS) with and without baseline deduction of (a)  $\beta$ -IR and (b) AmIR with IR-AQD. MFRDS with baseline deduction are shown with a translation on the vertical axis for clear. Each sample was characterized three times individually, and the corresponding nine MFRDS are shown here.

further study in this work. The a.d. and s.d. of IR solids and IR-AQD with themselves are small (Table S2,<sup>†</sup> a.d. < 0.03 and s.d. < 0.04). The a.d. and s.d. of the MFRDS of AmIR with IR-AQD are the smallest (0.031 and 0.059) among the four IR solids, and those of the MFRDS of IRD with IR-AQD are the smallest (0.052 and 0.084) among the three IR crystals.

### 3.2 MFRDS analysis of IR-DMSOD with IR solids

Considering that  $\beta$ -IR can be recrystallized from IR 70 vol% DMSO aqueous solution, the MFRDS analysis of IR in 70 vol% DMSO aqueous solution with IR solids was carried out here to explain this selective solution crystallization behavior. The MFRS of 70 vol% DMSO (DMSO) and saturated 70 vol% DMSO aqueous solution of IR (IR-DMSO) are shown in Fig. 3a. Because of the strong Raman signals of the DMSO/H<sub>2</sub>O mixed solvent (70 vol% DMSO), the observed Raman signals of IR are small peaks at 1450 and 1550  $\text{cm}^{-1}$ . The MFRS of solute IR in IR-DMSO (IR-DMSOD) was calculated by subtracting the Raman

Table 1 Summary of the average deviation (a.d.) and standard deviation (s.d.) of all the data in the MFRDS with and without baseline deduction of IR-AQD with four different IR solids. Each example was characterized three times individually, and the a.d. and s.d. were calculated from the corresponding nine MFRDS

MFRDS (300–1800 $\text{cm}^{-1}$ )	Without baseline deduction		With baseline deduction	
	a.d.	s.d.	a.d.	s.d.
$\alpha$ -IR with IR-AQD	0.080 (11)	0.123 (13)	0.070 (6)	0.107 (10)
$\beta$ -IR with IR-AQD	0.096 (16)	0.146 (14)	0.065 (4)	0.116 (7)
IRD with IR-AQD	0.077 (14)	0.109 (15)	0.052 (3)	0.084 (4)
AmIR with IR-AQD	0.086 (10)	0.104 (11)	0.031 (2)	0.059 (3)



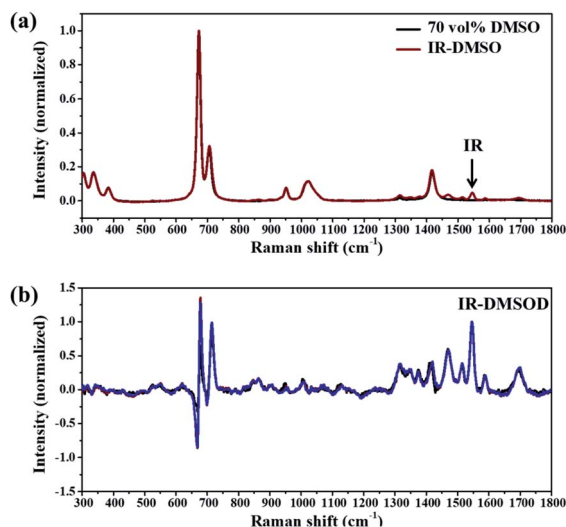


Fig. 3 MFRS of (a) 70 vol% DMSO aqueous solution (DMSO) and saturated 70 vol% DMSO aqueous solution of IR (IR-DMSO), (b) IR-DMSOD (the results of three parallel tests are shown here).

signal of the mixed solvent from the MFRS of IR-DMSO (Fig. 3b), which shows the signals originated from the interaction between IR molecules or IR and solvents molecules.

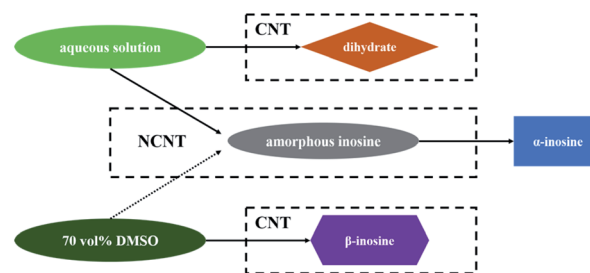
The MFRDS with baseline deduction analysis results of IR-DMSOD with the four different IR solids and itself (Tables 2 and S3, Fig. S4†) show that the a.d. and s.d. of the MFRDS of AmIR with IR-DMSOD (0.055 and 0.114) are the smallest among the four IR solids and those of the MFRDS of  $\beta$ -IR with IR-DMSOD (0.079 and 0.141) are the smallest among the three IR crystals. Since the strong Raman signals of solvent mainly appear in the range of 600–750  $\text{cm}^{-1}$ , we do the Raman difference spectra (RDS) analysis in the range of 800–1800  $\text{cm}^{-1}$  (Tables 2 and S3†) to eliminate the interference of solvent peaks. Similarly, the a.d. and s.d. of the RDS in the range of 800–1800  $\text{cm}^{-1}$  of AmIR with IR-DMSOD (0.046 and 0.068) are the smallest among the four IR solids and those of the RDS of  $\beta$ -IR with IR-DMSOD (0.077 and 0.119) are the smallest among the three IR crystals.

### 3.3 Explanation and prediction for the crystallization behaviour of IR solutions using MFRDS analysis

The selective crystallizations from IR solutions (IR-AQ and IR-DMSO) were explained and predicted by MFRDS analysis

(Scheme 2). The MFRDS analysis results indicate that the short-range orders of IR assemblies both in IR-AQ and IR-DMSO are most similar to AmIR, which is consistent with that amorphous phase is a supercooled liquid.<sup>17</sup> However, AmIR is not stable in solution and can easily transform to  $\alpha$ -IR *via* a possible NCNT process. The corresponding processes were observed in IR-AQ that AmIR can be obtained by spray drying at a high temperature 150 °C and  $\alpha$ -IR can be crystallized at room temperature. As DMSO is a kind of solvent with high boiling point, we cannot obtain AmIR from IR-DMSO by removing solvents quickly. However, we found that  $\alpha$ -IR can be crystallized from IR-DMSO when the solution was cooled from 60 °C to a lower temperature as  $-18$  °C (Fig. 4).  $\alpha$ -IR obtained from IR-DMSO might be transformed *via* an amorphous intermediate phase (as shown in Scheme 2). The MFRDS analysis results also indicate that the short-range orders of IR molecules in IR-AQ are most similar to those of IRD and IR-DMSO are most similar to  $\beta$ -IR among IR crystals, which are consistent with the phenomena that IRD can be obtained at a low temperature 10 °C from IR-AQ and  $\beta$ -IR can be obtained from IR-DMSO.

Generally, different polymorphs can crystallize from the same solution of organic molecules by controlling the experiment conditions. In this work,  $\alpha$ -IR (room temperature), IRD (a low temperature 10 °C), and AmIR (spray drying at a high temperature 150 °C) were obtained separately from IR-AQ easily by varying the temperature of IR-AQ. Similarly,  $\alpha$ -IR (room temperature) and  $\beta$ -IR ( $-18$  °C) can be crystallized separately from IR-DMSO by changing the cooling temperature of the saturated solution. Although  $\alpha$ -IR does not have the similar short-range orders with IR-AQD and IR-DMSOD, it can selectively crystallize from IR-AQ and IR-DMSO *via* a transformation



Scheme 2 Explanation for the selective crystallization from IR solutions (aqueous solution and 70 vol% DMSO aqueous solution) through MFRDS analysis. CNT refers to classical nucleation process and NCNT refers to non-classical nucleation process.

Table 2 Summary of the a.d. and s.d. of all the data in the MFRDS with baseline deduction in different ranges (300–1800  $\text{cm}^{-1}$  or 800–1800  $\text{cm}^{-1}$ ) of IR-DMSOD with four different IR solids. Each example was characterized three times individually, and the a.d. and s.d. were calculated from the corresponding nine MFRDS

MFRDS with baseline deduction	300–1800 $\text{cm}^{-1}$		800–1800 $\text{cm}^{-1}$	
	a.d.	s.d.	a.d.	s.d.
$\alpha$ -IR with IR-DMSOD	0.098 (6)	0.173 (13)	0.093 (5)	0.146 (6)
$\beta$ -IR with IR-DMSOD	0.079 (8)	0.141 (20)	0.077 (5)	0.119 (10)
IRD with IR-DMSOD	0.085 (7)	0.153 (18)	0.081 (2)	0.126 (3)
AmIR with IR-DMSOD	0.055 (7)	0.114 (23)	0.046 (2)	0.068 (2)



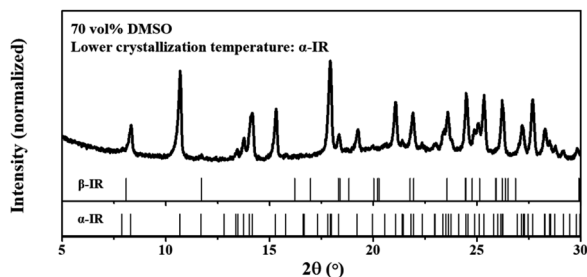


Fig. 4 PXRD pattern of the recrystallized product from saturated 70 vol% DMSO solution of IR (the solution was cooled from 60 °C to –18 °C).  $\beta$ -IR was prepared by cooling the solution from 60 °C to room temperature.

of AmIR precursor. It is also possible that different polymorphs can crystallize from different solutions. In this work, IRD and  $\beta$ -IR were obtained from IR-AQ and IR-DMSO respectively. When the a.d. and s.d. of the MFRDS of solutes in different solutions are quite large, you may conclude that solutes in different solutions separately have similar short-range orders with different solids. Thus, MFRDS analysis can not only be used for explicating the selective crystallization behavior in different solutions which have been observed, but can also be suitable for predicting the formations of new polymorphs of organic molecules in different solvents. This strategy has a huge application prospect in the area of drug polymorphs.

IR has good solubility in water ( $\alpha$ -IR, 3.29 g/100 g water at 30 °C) and DMSO aqueous solution ( $\alpha$ -IR, >5 g/100 g 70 vol% DMSO at 30 °C),<sup>12,15</sup> which ensures that its Raman signals are strong enough for further analysis. However, many organic molecules, including drugs, do not have good solubility in their recrystallization solvents, which would make it difficult to obtain the MFRDS and further influence the applications of this method in the nucleation processes analysis. Enhanced Raman technology may be helpful to break this limit.

## 4 Conclusions

MFRDS analysis of four solid phases and two solutions of IR were carried out in this work. The analysis results indicate that IR in aqueous solution has the similar short-range orders with AmIR and IRD, while IR in 70 vol% DMSO aqueous solution has the similar short-range orders with AmIR and  $\beta$ -IR. CNT processes including IRD obtained from IR-AQ and  $\beta$ -IR obtained from IR-DMSO and NCNT processes including AmIR obtained from IR-AQ and  $\alpha$ -IR obtained from IR-AQ and IR-DMSO via amorphous intermediate are proposed here to explain the experimental phenomena. Thus, MFRDS analysis is a feasible method to explain and predict the possible precipitation products from various solutions of small organic molecules.

## Abbreviation

### Analysis method/substance

LFRS Low-frequency Raman spectra

MFRS	Mid-frequency Raman spectra
RDS	Raman difference spectra
MFRDS	Mid-frequency Raman difference spectra
PXRD	Powder X-ray diffraction
UV-vis	Ultraviolet-visible spectroscopy
GR	Guanosine
AmGR	Amorphous guanosine
IR	Inosine
$\alpha$ -IR	$\alpha$ -Anhydrous inosine
$\beta$ -IR	$\beta$ -anhydrous inosine
IRD	Inosine dihydrate
AmIR	Amorphous inosine
IR-AQ	Saturated aqueous solution of IR
IR-AQD	Solute IR in IR-AQ and its MFRS
IR-DMSO	Saturated 70 vol% DMSO aqueous solution of IR
IR-DMSOD	Solute IR in IR-DMSO and its MFRS

## Conflicts of interest

There are no conflicts to declare.

## Acknowledgements

Financial support from the National Natural Science Foundation of China (Grant No. 22005175), the Natural Science Foundation of Fujian Province (Grant No. 2021J011116, 2021J011114), the Undergraduate Entrepreneurship Training Program of Fujian Province (S202011311062X) and Sanming University (19YG14) is gratefully acknowledged.

## Notes and references

- R. J. Davey, S. L. M. Schroeder and J. H. ter Horst, *Angew. Chem., Int. Ed.*, 2013, **52**, 2166–2179.
- D. Gebauer, M. Kellermeier, J. D. Gale, L. Bergström and H. Cölfen, *Chem. Soc. Rev.*, 2014, **43**, 2348–2371.
- G. C. Sosso, J. Chen, S. J. Cox, M. Fitzner, P. Pedevilla, A. Zen and A. Michaelides, *Chem. Rev.*, 2016, **116**, 7078–7116.
- X. Li, J. Wang, T. Wang, N. Wang, S. Zong, X. Huang and H. Hao, *Sci. China: Chem.*, 2021, **64**, 1460–1481.
- K. Berzinš, S. J. Fraser-Miller, T. Rades and K. C. Gordon, *Mol. Pharmaceutics*, 2019, **16**, 3678–3686.
- K. Berzinš, J. J. Sutton, S. J. Fraser-Miller, T. Rades, T. M. Korter and K. C. Gordon, *Cryst. Growth Des.*, 2020, **20**, 6947–6955.
- K. Berzinš, S. J. Fraser-Miller and K. C. Gordon, *Anal. Chem.*, 2021, **93**, 3698–3705.
- K. Berzinš, S. J. Fraser-Miller and K. C. Gordon, *Anal. Chem.*, 2021, **93**, 8986–8993.
- A. Jantschke, I. Pinkas, A. Hirsch, N. Elad, A. Schertel, L. Addadi and S. Weiner, *J. Struct. Biol.*, 2019, **207**, 12–20.
- M. C. Alvarez-Ros and M. Alcolea Palafox, *J. Mol. Struct.*, 2013, **1047**, 358–371.
- A. R. I. Munns and P. Tollin, *Acta Crystallogr., Sect. B: Struct. Crystallogr. Cryst. Chem.*, 1970, **26**, 1101–1113.
- S. Yoshihisa, *Bull. Chem. Soc. Jpn.*, 1974, **47**, 2549–2550.



- 13 Y. Shi, H. Zhang and X. Wang, *J. Chem. Eng. Data*, 2020, **65**, 2170–2177.
- 14 U. Thewalt, C. E. Bugg and R. E. Marsh, *Acta Crystallogr., Sect. B: Struct. Crystallogr. Cryst. Chem.*, 1970, **26**, 1089–1101.
- 15 S. Yoshihisa and H. Kentaro, *Bull. Chem. Soc. Jpn.*, 1974, **47**, 2551–2552.
- 16 R. A. Chiarella, A. L. Gillon, R. C. Burton, R. J. Davey, G. Sadiq, A. Auffret, M. Cioffi and C. A. Hunter, *Faraday Discuss.*, 2007, **136**, 179–193.
- 17 T. E. Gartner, *Proc. Natl. Acad. Sci. U. S. A.*, 2021, **118**, e2112191118.

